

A Joint Statistical and Dynamical Assessment of Atmospheric Response to North Pacific Oceanic Variability in CCSM3

YAFANG ZHONG AND ZHENGYU LIU

Center for Climatic Research, University of Wisconsin—Madison, Madison, Wisconsin

(Manuscript received 16 August 2007, in final form 24 April 2008)

ABSTRACT

Atmospheric response to North Pacific oceanic variability is assessed in Community Climate System Model, version 3 (CCSM3) using two statistical methods and one dynamical method. All methods identify an equivalent barotropic low response to a warmer sea surface temperature (SST) anomaly in the Kuroshio Extension region (KOE) during early–midwinter. While all three methods capture the major features of the response, the generalized equilibrium feedback assessment method (GEFA) isolates the impact of KOE SST from a complex context, and thus makes itself an excellent choice for similar practice.

1. Introduction

The effect of midlatitude oceanic variability on the atmosphere is a key to understanding and predicting extratropical low-frequency climate variability. The large ensembles of atmospheric general circulation model (AGCM) simulations in the 1990s suggest that the extratropical ocean is able to influence the atmosphere beyond the local air–sea adjustment (Barsugli and Battisti 1998) but with modest strength compared to internal atmospheric variability (Kushnir et al. 2002). In the meantime, the AGCMs showed a large disparity of the atmospheric response. Since the late 1990s, an increasing effort has been made to assess atmospheric response to extratropical SST in the real world (Frankignoul et al. 1998; Czaja and Frankignoul 2002; Liu et al. 2006; Frankignoul and Sennechael 2007). Frankignoul et al. (1998) proposed a simple statistical method for the assessment of atmospheric quasi-equilibrium response to the midlatitude oceanic variability. Their method is based on the key fact that the ocean cannot be forced by internal atmospheric variability of later time. The atmospheric response thus should be assessed using the SST lead, rather than the simultaneous, ocean–atmosphere covariance. This statistical method

is termed the equilibrium feedback assessment (EFA) in Liu et al. (2008) and has been widely used to determine large-scale atmospheric response to midlatitude SSTs. A combination of the EFA with maximum covariance analysis (MCA) enabled Czaja and Frankignoul (2002) to conclude that North Atlantic SST anomalies could induce significant atmospheric response during wintertime. Employing the same strategy, Liu et al. (2006) and Frankignoul and Sennechael (2007) found that North Pacific SST anomalies have a substantial impact on the extratropical atmosphere during certain seasons. In consistent, a straightforward EFA application by Liu and Wu (2004) suggests that the Kuroshio Extension region (KOE) SST variability may force an equivalent barotropic high over the Aleutian low.

Since the ultimate goal is to identify the atmospheric response in the real world, and since present general circulation models (GCMs) are imperfect, the statistical method is critical. In the meantime, the statistical method needs to be improved because of its limitations associated with various assumptions. When the EFA method is used to assess atmospheric dynamic response to a single index of localized SST variability, the interpretation of the result is problematic, because covarying SST elsewhere could also affect the response, and therefore the contribution from different SST regions becomes unclear. The combination with MCA is able to identify the leading SST forcing and atmospheric response modes. However, these MCA results depend

Corresponding author address: Y. Zhong, CCR, 1225 W. Dayton St., Madison, WI 53706.
E-mail: yafangzhong@wisc.edu

not only on the atmospheric response sensitivity, but also on the SST variability in the coupled system. Recently, Liu et al. (2008) proposed the generalized EFA (GEFA) method that is essentially a multivariate generalization of the original EFA. The GEFA directly assesses the atmospheric response that is independent of the pattern of SST evolution. It allows for the assessment of the atmospheric response to localized SST anomaly in interested regions, which is highly desirable in the mechanism study and prediction of low-frequency climate variability. Furthermore, it is important to validate the statistical method in a complex ocean–atmosphere system, such as a GCM, against the true response that is obtained using explicit dynamic experiments. This has prompted us to take a joint statistical and dynamical approach, which has shown promising results (Liu and Wu 2004; Liu et al. 2007).

The purpose of this work is twofold. First, it attempts to assess the atmospheric response to North Pacific oceanic variability in Community Climate System Model, version 3 (CCSM3) using advanced statistical and dynamical methods. The focus is the atmospheric dynamic response to KOE SST variability for its important role in the Pacific low-frequency climate variability (Kwon and Deser 2007; Zhong et al. 2008). Second, it serves as a systematic demonstration of the performance of various methods for the assessment of the response, and calibrates the new statistical method, that is, GEFA, against other methods. A joint statistical and dynamical assessment is performed and identifies a robust warm SST low response of modest amplitude with respect to KOE SST during early–midwinter. This work suggests the power of the joint statistical and dynamical approach for the assessment of the atmospheric response. The consistency of the statistical methods with the dynamical approach lends credence to their application to the observation.

2. The model

CCSM3 is a state-of-art global climate model (Collins et al. 2006). For this study, $T31 \times 3$ resolution (Yeager et al. 2006) is employed. The atmospheric component of CCSM3 at $T31 \times 3$ is the Community Atmosphere Model, version 3 (CAM3) at T31 resolution, which has 26 levels in vertical. The ocean model is the Parallel Ocean Program (POP) version 1.4.3 in spherical polar coordinates with a dipole grid and has a nominal horizontal resolution of 3° . The vertical dimension is a depth coordinate with 25 levels extending to 4.75 km. Under the present-day climate conditions, CCSM3 has been integrated for 880 yr without flux adjustment,

showing no apparent climate drift. It has similar model climatology to higher-resolution CCSM3 and simulates a reasonable North Pacific climate variability (Zhong et al. 2008).

To minimize the interference of tropical climate variability, all the statistical analyses and dynamical experiments are based on an extratropical control run that decouples the tropical climate system equatorward of 20° (where the SST boundary condition for the atmospheric model component is prescribed as monthly climatology) and hence suppresses virtually all its variability. Compared to traditional statistical removal of tropical influence, this dynamical operation has the advantage of clearly isolating the tropical climate variability and its teleconnective impact (Liu et al. 2006; Frankignoul and Sennechael 2007). This extratropical control run starts from an equilibrium state of the standard CCSM3 simulation at year 651 and is integrated for 400 yr yielding similar climatology and North Pacific climate variability to the latter (Zhong et al. 2008).

3. Preliminary evidence of atmospheric response to the North Pacific Ocean

For the first clue of air–sea interaction in the North Pacific, we calculated the lagged correlation as a function of calendar month between regional SST and sea level pressure (SLP) for the KOE region (35° – 45° N, 140° – 180° E; Fig. 1a). It shows a strong asymmetry with lag, with a higher correlation at negative lags (SLP leads). This asymmetry suggests the predominance of atmospheric forcing on the ocean in the air–sea interaction (Frankignoul and Hasselmann 1977). With the atmosphere leading, the largest positive correlation occurs in summer half year when SST is most responsive to atmospheric forcing due to the shallow mixed layer; it exhibits little correlation in wintertime, indicating the possible control of KOE SST by nonlocal oceanic dynamics (Schneider et al. 2002; Mochizuki and Kida 2006). When the SST leads, significant correlation appears only in early–midwinter, implying a seasonal dependence of atmospheric response. The negative correlation suggests a warmer KOE SST during early–midwinter tends to force a low SLP. The significant correlation at long SST leads is associated with the long persistence of SST.

Similar results are obtained for the lagged correlation between KOE SST and SLP over the central North Pacific (CNP; 35° – 45° N, 180° E– 140° W; Fig. 1b). The maximum positive correlation when the atmosphere leads SST by 1 month reflects a basinwide SLP forcing that is associated with variability in the Aleutian low

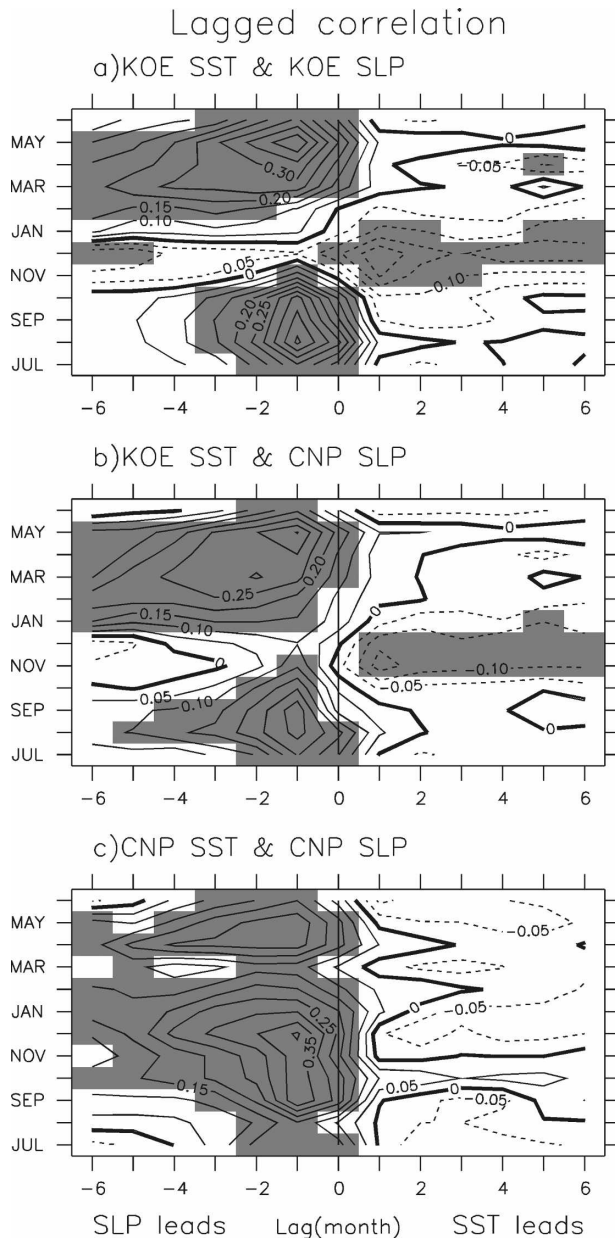


FIG. 1. Lagged correlation between (a) KOE SST and KOE SLP, (b) KOE SST and CNP SLP, and (c) CNP SST and CNP SLP. The ordinate is the SLP calendar month, while the abscissa is the lag. Positive lags indicate SST lead of SLP and negative lags SLP. For example, the maximum positive correlation in (c) corresponds to CNP SST in January and CNP SLP in December. The correlation significant at 95% is shaded.

(Liu et al. 2007). The marked negative correlation at the SST leading serves as a hint of large-scale atmospheric response to KOE SST beyond its local impact.

It should be mentioned that the modeled air–sea interaction differs substantially from the observed. For example, the model shows maximum atmospheric in-

duced correlation in spring and summer, in sharp contrast to wintertime from the observation (Liu et al. 2007). Also deviated from the observation is the significant negative correlation at SST leading that appears only in early–midwinter, when the observation exhibits weak positive correlation as a hint of positive oceanic feedback to atmosphere (Liu et al. 2007). However, this model deficiency is not a problem for the present study in that, our objective is to compare the performance of dynamical and statistical approaches in CCSM3 application, not to calibrate the model behavior against observation.

4. EFA assessment

To further quantify the response, we apply EFA method to the extratropical control run. EFA was proposed by Frankignoul et al. (1998) in an attempt to estimate the SST–turbulent heat flux feedback, and has been applied to multiple studies of feedbacks between different climate variables (Czaja and Frankignoul 2002; Liu and Wu 2004; Liu et al. 2007; Notaro et al. 2006). It assumes a linear relation between a fast atmosphere field and a slow ocean field, the geopotential height (GHT) and SST anomaly in our case: the GHT variability $h(t)$ consists of two parts, the predictable part given a predictable SST $s(t)$, being a linear function of $s(t)$, and the unpredictable part associated with atmospheric internal variability $n(t)$; that is,

$$h(t) = bs(t) + n(t). \quad (1)$$

Following Liu et al. (2008), b is the parameter calibrating the quasi-equilibrium GHT response to SST anomaly. In estimating b , rather than instantaneous GHT/SST covariance, the SST lead covariance is used to annihilate the estimate error introduced by the atmospheric noise forcing that is hard to reduce otherwise. The response parameter b is thus estimated as

$$b = \langle h(t), s(t - \tau) \rangle / \langle s(t), s(t - \tau) \rangle, \quad (2)$$

where angle bracket denotes the cross covariance and τ is a SST leading time that is longer than the damping time scale of the atmosphere.

SST influence on the atmosphere is strongly seasonal dependent (Peng et al. 1997; Czaja and Frankignoul 2002; Liu et al. 2006; Frankignoul and Sennechael 2007). EFA is used to illustrate the seasonal evolution of the response averaged over 30° – 60° N, 140° E– 140° W to KOE SST. The most outstanding feature in Fig. 2 (upper) is the seasonal contrast between early–midwinter and the remainder of the year. The response during the former is characterized by an equivalent barotropic low with magnitude at the surface that

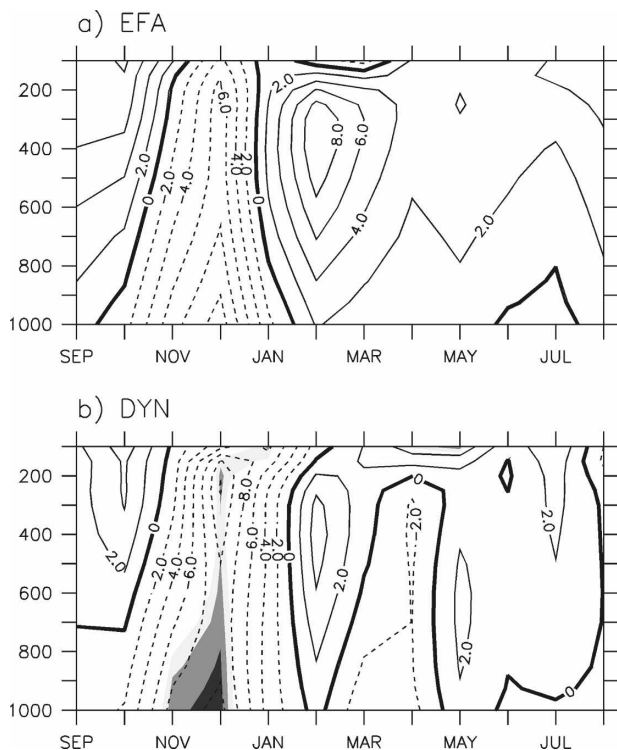


FIG. 2. Seasonal evolution of GHT response (averaged over 30° – 60° N, 140° E– 140° W) to KOE SST for (top) EFA and (bottom) dynamical assessments. Contour interval is $2 \text{ m } ^{\circ}\text{C}^{-1}$. Shading indicates the response of dynamical assessment statistically significant at 95%, 90%, and 85% levels.

barely reaches $10 \text{ m } ^{\circ}\text{C}^{-1}$. Even smaller response is found in the remainder of the year, appearing as an equivalent barotropic high. This result is consistent with the lagged correlation in section 3.

Spatial structure of the response to KOE SST during November–December is then examined. We focus on the local response over the North Pacific (20° – 65° N, 100° E– 100° W). The response is first estimated for November and December, respectively, at lag 1 and 2 months; shown in Figs. 3a,b is an average of both months at the two lags. Consistently, it reveals an equivalent barotropic low response over the Aleutian low region, with a southwest–northeast orientation. The maximum low response is over $15 \text{ m } ^{\circ}\text{C}^{-1}$ for both levels, a modest perturbation on the background of strong internal variability. These maxima have comparable magnitude with those of observed barotropic ridge response, especially for 850 hPa (Liu et al. 2007).

As pointed out by Liu et al. (2008), the EFA estimation assumes a linear atmosphere response to the SST forcing in the KOE region only; this might not be true for CCSM3, since the CNP SST also influences the atmosphere through heat flux (Zhong et al. 2008). In the

next section, dynamic approach is invoked to provide a truth calibration for the EFA assessment.

5. Dynamical assessment

Following Liu and Wu (2004), ensemble simulation is performed on the basis of the extratropical control run. The design of the simulation follows Liu et al. (2007). The ensemble simulation has 100 members; each starts from a September model state selected from the extratropical control run in successive years. For each ensemble member, a bell-shaped temperature anomaly is added to the model temperature at the initial time step, extending uniformly from surface down to 400 m. It has a maximum of 2°C and an average of 1.2°C in the KOE region. This coupled model is then left to evolve freely during a 24-month integration. The subsurface temperature anomaly here is to simulate an oceanic source for the KOE SST variability. Because of a slow damping of the subsurface anomaly, the KOE SST anomaly shows little reduction from the first year to the second.

The ensemble simulation produces a distinguished seasonal cycle of GHT response (Fig. 2, lower), derived as an average of the ensemble mean for years 1 and 2. Most striking is the equivalent barotropic low response during early–midwinter, reminiscent of the EFA result. Furthermore, the magnitude of response is slightly larger than that from the EFA estimation. The agreement between the two methods is less clear for other seasons. The response polarity is opposite for summer when the response is weakest; or, the response magnitude hardly matches while both get the same sign, as in February. The comparison of the two methods is consistent with the lagged correlation (Fig. 1), which suggests significant response only in early–midwinter. For comparison, the similar studies by Liu and Wu (2004) and Liu et al. (2007) found a barotropic high response in early–midwinter, using the Fast Ocean Atmosphere Model (FOAM). The discrepancy may be related to the different background states in FOAM and CCSM3 (Peng et al. 1997).

The GHT response in November–December has a spatial structure largely similar to that identified by EFA, featuring an overall intensification of Aleutian low system (Figs. 3c,d). The response amplitude is also comparable with maxima over $15 \text{ m } ^{\circ}\text{C}^{-1}$ for 850 hPa and over $20 \text{ m } ^{\circ}\text{C}^{-1}$ for 250 hPa. Some differences from EFA result can also be noticed. For instance, the geopotential anomaly has an opposite sign over East Asia and the most northern region of the interested domain. The discrepancy may relate to the influence of local surface condition aside from the KOE SST, or nonlinear atmospheric responses that cannot be captured by

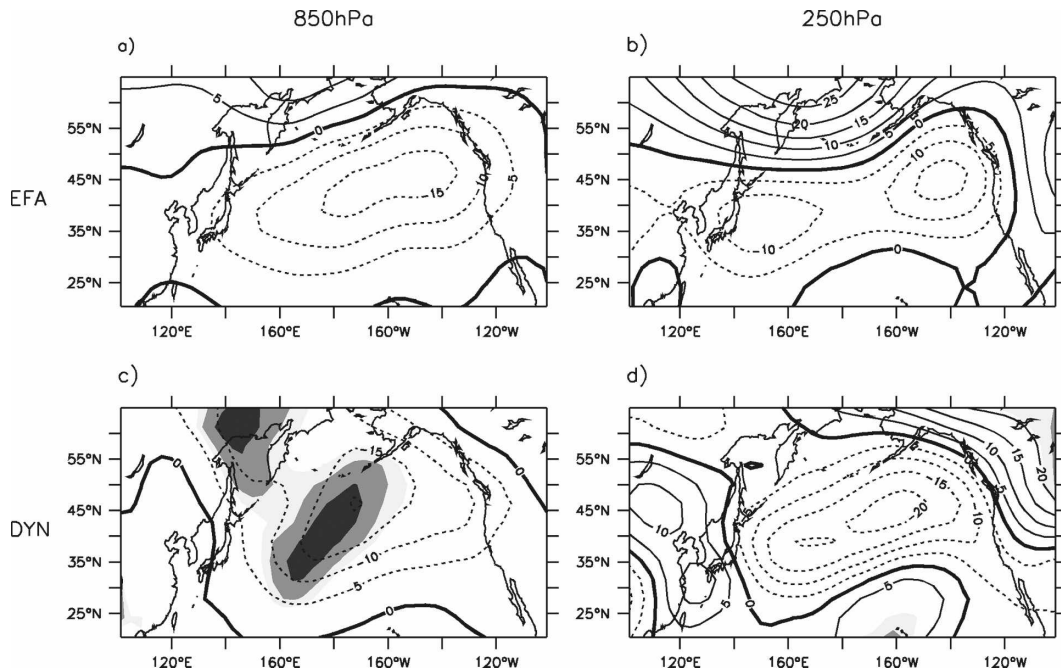


FIG. 3. Estimation of GHT response to KOE SST during November–December at (left) 850 hPa and (right) 250 hPa using (a), (b) EFA and (c), (d) dynamical methods. Contour interval is $5 \text{ m } ^\circ\text{C}^{-1}$. The EFA result is calculated as an average of the response at lag 1 and 2 months. Response of dynamical assessment statistically significant at 95%, 90%, and 85% levels is shaded.

the linear EFA methods (Liu et al. 2008). To gain some insight into the discrepancy, we proceed to estimate the response with an improved EFA.

6. GEFA assessment

In light of the limitation of EFA, Liu et al. (2008) proposed a new statistical method, essentially generalizing EFA for the detection of multisource response. The GEFA has done a decent job identifying responses in a simple idealized model, yet its performance in more complex context such as the observation or GCMs remains to be seen. In principle, it fits well for the objective of detecting atmospheric response in complex GCMs or the observation, where the atmosphere over North Pacific could respond to SST variability outside the KOE region. Here, we perform the GEFA in the SST rotated EOF (REOF) space, to study the response to SST anomaly in different parts of the North Pacific Ocean. The generalization of (1) can be written in the vector form

$$\mathbf{H}(t) = \mathbf{B}\mathbf{S}(t) + \mathbf{N}(t), \quad (3)$$

where $\mathbf{H}(t)$ is the geopotential height field of I points consisting of all the atmospheric grids over North Pacific, $\mathbf{S}(t)$ is the SST field of J points corresponding to

the leading J modes from REOF analysis of SST, $\mathbf{N}(t)$ is the atmospheric internal variability, element b_{ij} of the response matrix \mathbf{B} represents the impact of the j th REOF of North Pacific SST on the i th atmospheric grid point. In analogy to (2), response matrix \mathbf{B} is estimated as

$$\mathbf{B}(\tau) = \mathbf{C}_{\text{HS}}(\tau)\mathbf{C}_{\text{SS}}^{-1}(\tau), \quad (4)$$

where $\mathbf{C}_{\text{HS}}(\tau)$ denotes the lagged cross-covariance matrices between GHT and SST, and $\mathbf{C}_{\text{SS}}(\tau)$ the auto-covariance matrices of SST. The response during November–December is calculated as an average of both months at lag 1 and 2, similar to the EFA estimation in section 4.

For winter response, the REOF analysis is performed with North Pacific SST ($20^\circ\text{--}60^\circ\text{N}$, $120^\circ\text{E}\text{--}100^\circ\text{W}$) averaged for November–February. Results are very similar when SST during October–March is used. The varimax rotation is applied to the leading 15 SST EOF modes. The resultant REOFs are then projected onto monthly SST data, and yield the corresponding monthly time coefficients to input as SST time series in (3). The estimate response is insensitive to the truncation of REOFs included in the GEFA calculation up to 10 modes. For the results shown here, the leading 8 modes are used explaining totally 67.2% of North Pa-

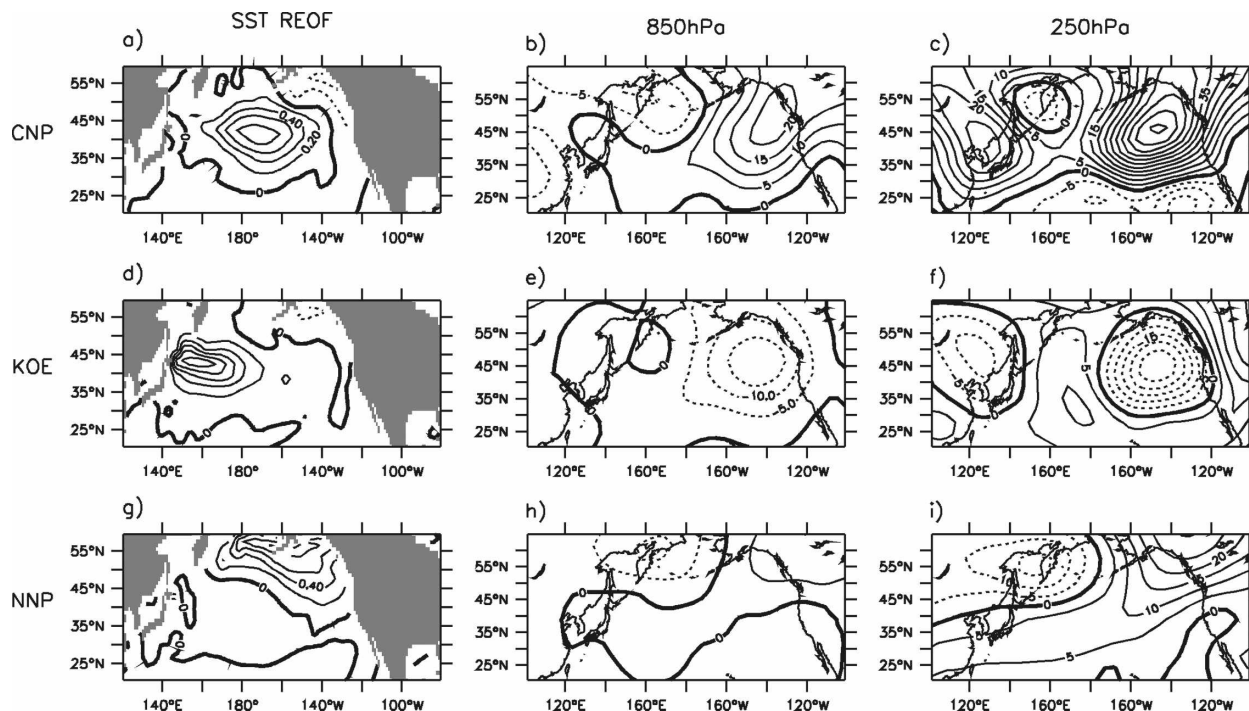


FIG. 4. (left) GHT response to leading three REOFs of North Pacific SST during November–December as estimated with GEFA methods. Response at (middle) 850 hPa and (right) 250 hPa is given for (a) REOF1 the CNP SST mode in (b), (c); (d) REOF2 the KOE mode in (e), (f); and (g) REOF3 the NNP mode in (h), (i). Contour interval is $5 \text{ m } ^\circ\text{C}^{-1}$.

cific SST variance. The three leading REOFs account for 13.3%, 11.2%, and 9.96% of the total variance, respectively, each being a regional SST mode with loading center at CNP, KOE, and northern North Pacific (NNP) by order (Fig. 4).

Response to the KOE SST mode is a downstream low with an equivalent barotropic structure. The maxima over the Aleutian low have amplitudes comparable with previous assessments, over $15 \text{ m } ^\circ\text{C}^{-1}$ for 850 hPa and $25 \text{ m } ^\circ\text{C}^{-1}$ for 250 hPa. A nonnegligible difference is the much weaker response over the western half of North Pacific basin (Figs. 4e,f) compared with EFA and dynamical results (Fig. 3). The CNP SST mode has a distinct impact, forcing a downstream barotropic high (Figs. 4b,c). This implies a critical dependence of atmospheric response to the location of SST forcing. Unlike the response to KOE SST, this downstream high amplifies with height, from over $20 \text{ m } ^\circ\text{C}^{-1}$ at 850 hPa to over $50 \text{ m } ^\circ\text{C}^{-1}$ at 250 hPa. The downstream high in responding to the NNP SST mode shares this feature, but has much weaker amplitudes for both levels (Figs. 4h,i). Albeit in a crude sense, the consistency with the univariate EFA and dynamical assessments concerning response to KOE SST suggests a reasonable performance of GEFA in a complex context. A more quantitative intercomparison is yet to be made,

more specifically, a reconstruction of the EFA response or dynamical assessment using GEFA response patterns. As illuminated in Liu et al. (2008), the EFA-derived response is in effect the outcome of both KOE SST and covarying SST forcing in other regions. A regression pattern with the base point of KOE SST (Fig. 5a) resembles the Pacific decadal oscillation (PDO; Mantua et al. 1997), exhibiting a like-sign anomaly in KOE and CNP and an opposite sign to the surroundings. Therefore, the EFA response may be better represented with a linear combination of all three GEFA response patterns in Fig. 4, rather than the KOE response pattern only. Similar argument can be applied to the response in dynamical assessment, for the significant SST anomaly also exists in CNP and NNP other from KOE (Fig. 5b).

7. Summary

The atmospheric response to the North Pacific oceanic variability is estimated with two statistical methods and a dynamical method. All three methods capture the major feature of the response: an equivalent barotropic low in responding to a warm KOE SST during early-midwinter. Some discrepancy in the response pattern is revealed by the intercomparison of these methods. It

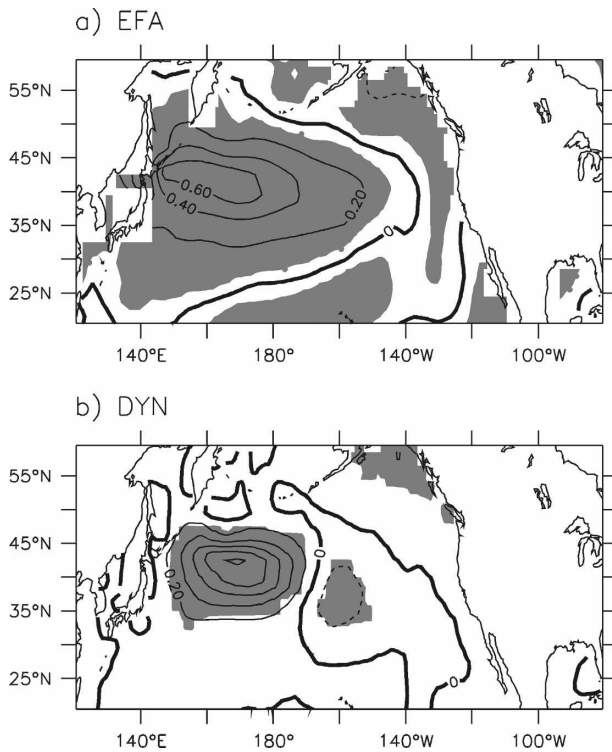


FIG. 5. Effective SST forcing pattern during November–December in (a) EFA and (b) dynamical assessments. (a) SST regression pattern with the base point of KOE SST, using output from the extratropical control run. (b) SST anomaly derived as the difference field between ensemble simulation and extratropical control run. Contour interval is 0.2°C . Shading indicates (a) regression coefficient and (b) SST anomaly that is statistically significant at 95% confidence level.

relates to the deficiency of the univariate EFA and dynamical methods failing to distinguish the response to KOE SST from the SST in other regions. In comparison, the GEFA better isolates the impact of KOE SST. The revealed atmospheric response implies large-scale air–sea coupling in the extratropics, which may give arise to the Pacific decadal-to-multidecadal variability in the CCSM3 (Zhong et al. 2008).

The warm-low response to North Pacific SST in CCSM3 differs from the warm-ridge response in many high-resolution models (Kushnir et al. 2002) and the observation (Liu et al. 2007). Yet, this warm-low response is not uncommon. Similar response has been reported to occur in other GCM simulations (Kushnir et al. 2002) and in the CCSM2 at T42 resolution (Kwon and Deser 2007). Therefore, the warm-low response is unlikely a product of low resolution, but the physics of the model. The atmospheric response to SST variability essentially involves interaction between the mean flow and transient eddies (Peng et al. 1997; Ferreira and Frankignoul 2005). The successful simulation of atmo-

spheric response thus hinges on the realistic reproduction of mean flows, transient eddies, and their interactions. The model biases in these aspects, as documented by Hurrell et al. (2006) and Alexander et al. (2006), may lead to an unrealistic representation of atmospheric response.

Although the tropical teleconnective impact is not directly addressed in the present study (recall the removal of tropical variability instead of the teleconnective impact itself), it remains a challenging yet important issue for detection of atmospheric response in observation or fully coupled GCM simulation. The GEFA provides a promising solution, for it can be readily applied in the presence of tropical influence (Liu et al. 2008). It is also important to better understand the physical mechanism for the tropical teleconnection to influence the midlatitude oceanic feedback to the atmosphere, possibly through modulation of background mean flow. All these issues remain to be studied in the future.

Acknowledgments. This work is supported by DOE and NOAA. We thank Na Wen and Yun Liu for useful discussion and Mark Marohl for editorial help. We also thank anonymous reviewers for their valuable comments and thoughtful suggestions.

REFERENCES

- Alexander, M., and Coauthors, 2006: Extratropical atmosphere–ocean variability in CCSM3. *J. Climate*, **19**, 2496–2525.
- Barsugli, J. J., and D. S. Battisti, 1998: The basic effects of atmosphere–ocean thermal coupling on midlatitude variability. *J. Atmos. Sci.*, **55**, 477–493.
- Collins, W. D., and Coauthors, 2006: The Community Climate System Model version 3 (CCSM3). *J. Climate*, **19**, 2122–2143.
- Czaja, A., and C. Frankignoul, 2002: Observed impact of Atlantic SST anomalies on the North Atlantic oscillation. *J. Climate*, **15**, 606–623.
- Ferreira, D., and C. Frankignoul, 2005: The transient atmospheric response to midlatitude SST anomalies. *J. Climate*, **18**, 1049–1067.
- Frankignoul, C., and K. Hasselmann, 1977: Stochastic climate models 2. Application to sea-surface temperature anomalies and thermocline variability. *Tellus*, **29**, 289–305.
- , and N. Sennechael, 2007: Observed influence of North Pacific SST anomalies on the atmospheric circulation. *J. Climate*, **20**, 592–606.
- , A. Czaja, and B. L’Heveder, 1998: Air–sea feedback in the North Atlantic and surface boundary conditions for ocean models. *J. Climate*, **11**, 2310–2324.
- Hurrell, J. W., J. J. Hack, A. S. Phillips, J. Caron, and J. Yin, 2006: The dynamical simulation of the Community Atmosphere Model version 3 (CAM3). *J. Climate*, **19**, 2162–2183.
- Kushnir, Y., W. A. Robinson, I. Blade, N. M. J. Hall, S. Peng, and R. Sutton, 2002: Atmospheric GCM response to extratropical SST anomalies: Synthesis and evaluation. *J. Climate*, **15**, 2233–2256.
- Kwon, Y., and C. Deser, 2007: North Pacific decadal variability in

- the Community Climate System Model version 2. *J. Climate*, **20**, 2416–2433.
- Liu, Q. Y., N. Wen, and Z. Y. Liu, 2006: An observational study of the impact of the North Pacific SST on the atmosphere. *Geophys. Res. Lett.*, **33**, L18611, doi:10.1029/2006GL026082.
- Liu, Z. Y., and L. X. Wu, 2004: Atmospheric response to North Pacific SST: The role of ocean–atmosphere coupling. *J. Climate*, **17**, 1859–1882.
- , Y. Liu, L. X. Wu, and R. Jacob, 2007: Seasonal and long-term atmospheric responses to reemerging North Pacific Ocean variability: A combined dynamical and statistical assessment. *J. Climate*, **20**, 955–980.
- , N. Wen, and Y. Liu, 2008: On the assessment of non-local climate feedback. Part I: the generalized equilibrium feedback assessment. *J. Climate*, **21**, 134–148.
- Mantua, N. J., S. R. Hare, Y. Zhang, J. M. Wallace, and R. C. Francis, 1997: A Pacific interdecadal climate oscillation with impacts on salmon production. *Bull. Amer. Meteor. Soc.*, **78**, 1069–1079.
- Mochizuki, T., and H. Kida, 2006: Seasonality of decadal sea surface temperature anomalies in the northwestern Pacific. *J. Climate*, **19**, 2953–2968.
- Notaro, M., Z. Liu, and J. W. Williams, 2006: Observed vegetation–climate feedbacks in the United States. *J. Climate*, **19**, 763–786.
- Peng, S. L., W. A. Robinson, and M. P. Hoerling, 1997: The modeled atmospheric response to midlatitude SST anomalies and its dependence on background circulation states. *J. Climate*, **10**, 971–987.
- Schneider, N., A. J. Miller, and D. W. Pierce, 2002: Anatomy of North Pacific decadal variability. *J. Climate*, **15**, 586–605.
- Yeager, S. G., C. A. Shields, W. G. Large, and J. J. Hack, 2006: The low-resolution CCSM3. *J. Climate*, **19**, 2545–2566.
- Zhong, Y. F., Z. Liu, and R. Jacob, 2008: Origin of Pacific multi-decadal variability in Community Climate System Model version 3 (CCSM3): A combined statistical and dynamical assessment. *J. Climate*, **21**, 114–133.